# Ab Initio Study of The Electronic Properties of The Quaternary Compounds $AgFeSnS_4$, $Ag_2KPS_4$ and $Ag_2KSbS_4$

**Omehe N. N.**

omehenn@fuotuoke.edu.ng

D.O.I: 10.56201/ijccp.v9.no4.2023.pg87.99

***Abstract***

*$AgFeSnS_4$, $Ag_2KPS_4$ and $Ag_2KSbS_4$ are quaternary materials with the stannite structure, and their electronic properties have been investigated via DFT using the pseudopotential method. The technique used was DFT+U with the Projector Augmented Wave (PAW). For exchange and correlation, the Generalised Gradient Approximation (GGA) was used. The calculations predicted $AgFeSnS_4$ to have semimetallic property with an intermediate Band (IB) of energy width of about 1.0 eV. The IB is sandwich between an intra valence band gap of 1.0 eV and an intra conduction band of 0.2 eV. $Ag_2KPS_4$ was predicted to have semiconducting property with a direct band value 0f 2.19 eV. $Ag_2KSbS_4$ was also predicted to be a semiconductor with a direct band gap value of 1.67 eV, both materials have their band gap at the Γ point of high symmetry. The partial density of states (PDOS) calculation showed that S-3p and Sn-5s dominated IB, Sn-5s dominated the conduction band for $AgFeSnS_4$. For $Ag_2KPS_4$, the top valence subband is mainly S-3p while P-3p dominated the bottom of the conduction band. The calculation also showed that $Ag_2KSbS_4$ has its top valence band dominated by S-3p while the conduction band bottom was mainly of Sb-4d and Sb-5s.*

***Keywords:*** *Quaternary materials, Intermediate Band, DFT+U, Semiconductor materials.*

## INTRODUCTION

Quaternary Chalcogenide are gaining a lot of attention from the research community due to its earth abundance, non toxic nature, and its technological applications. $AgFeSnS_4$, $Ag_2KPS_4$ and $Ag_2KSbS_4$ belongs to a large family of quaternary compound with applications in non linear and linear optical devices (Huang et al., 2017), thiophosphates and thioantimonates are suitable for superionic conductors (Lange et al., 2023). They charge transport, Hydrogen storage and in Li batteries (Fuentealba et al., 2020), and hydrogen evolution reaction (Coleman et al., 2022). Not much has been done on Ag containing quaternary compounds when compared to that of Cu. Some of the previous works on these materials include experimental and theoretical investigations Brunetta et al., (2012), studied the electronic structure of the diamond-like semiconductor $Ag_2ZnSiS_4$. The crystals were grown by solid state synthesis, a monoclinic phase (Pn) with Lattice

parameters a = 6.4052 Å, b = 6.5484 Å, c = 7.934Å, and β = $90.455^0$ was reported. Their optical diffuse reflectance spectroscopic analysis yielded a band gap of 3.28 eV. Also, their DFT computation predicted a band gap of 1.88 eV similarly, Moroz et al., (2020), prepared samples of compound in the system Ag-Fe-Sn-S via solid state synthesis and reported of their thermodynamic properties.

Caye et al., (1968) had earlier study the mineral Hocartite, naturally occurring $Ag_2FeSnS_4$ Compound, using electron miscroprobe, they reported a stannite structure having lattice parameters a = 5.74 Å, c = 10.96 Å. Wu et al., (2009) prepared samples of $Ag_2Nb(P_2S_6)(S_2)$ and $kAg_2(PS_4)$ by the reaction of $K_2S_3$, Ag, Nb, $P_2S_3$ with sulphur powder. Analysis was by UV-visable diffused reflectance spectroscopy. A stannite structure with lattice parameters a = 6.6471 Å, c = 8.1693 Å and z = 2 were reported. Schimek et al., (1996), prepared four samples of alkali metal of silver (Ag) antimony sulphides $MAg_2SbS_4$ and $M_2AgSbS_4$ (M = K, Rb). the samples were grown via sepercritical Ammonia, the lattice parameter a = 6.886 Å and c = 8.438 Å and z = 2 were reported. Samples of $Cu_2PbSiS_4$, $Ag_2PbGeS_4$, and $kAg_2SbS_4$ were grown by Nhalil et al., (2018) using high temperature synthesis. Their optical diffuse reflectance study yield a band gap value range of 1.6 eV-1.8 eV for the three semiconductors. A DFT study was also carried out which indicated that the materials have indirect band gaps. A mineral Toyohaite close to Hocartite with a formula $Ag_2FeSn_2S_8$ have been reported in the literature (Yajima et al., 1991). Other phases of Thiophosphates have been reported in the literature (Fuenteaiba et al., (2020).

Theoretically, Rasukkannu et al., (2017) investigate the electronic properties of several bulk materials including $AgKSbS_4$. The pseudopotential method was applied in the investigation, for exchange and correlation, the generalized gradient approximation (GGA) was used. They reported an indirect band gap of 0.81 eV and an intermediate band gap with of 0.94 eV. Using the full potential linearized augmented plane wave plus local orbitals methods, Berri et al., (2019) investigated the structural, electronic, optical, and thermodynamic properties of $Ag_2KSbS_4$. The GGA was used for exchange and correlation as parametrized by both perdew-Burke-Ernerhof (PBE) and Engel Vosko (EV). The reported lattice parameter are a = 6.912 Å, c = 8.490 Å. Huang et al., (2017) studied the effect of $(PS4)^{-1}$ anion on the optical properties of Silver containing potassium thiophosphates.

In this research, the DFT+U method will be applied to investigate the electronic properties of $Ag_2SnS_4$, $Ag_2KPs_4$ and $Ag_2KSbS_4$ compounds.

**Computational details**

$Ag_2FeSnS_4$, $AgKPS_4$, and $Ag_2KSbS_4$ are tetragonal structured materials crystallizing in the I-42m space group. The silver atom (Ag) occurs the 4d Wyckoff's atomic site, iron (Fe) and potassium occur the 2a site, Tin (Sn), and potassium occur the 2a site; Tin (Sn), phosphorus and Antimony (Sb) occur the 2b site, while sulphur occurs the 8i site. The total number of atoms in the unit cell is 16 atoms, since there are two formula unit (that is, a z-value of two) in one unit cell. The computations were performed using the Abinit software package (Gonze et al., 2002; Gonze et al., 2005), this package implements the Pseudopotential method used in ab-initio methods for material properties computations. In this work, the electronic band structures, the total density of states

(DOS), and the partial density of states for the materials under investigation was carried out. The GGA+U method with the projector augmented wave was used in all calculations. A tolerance of $10^{-10}$ Ha/Br was applied to the ground state calculations. A kinetic cutoff energy of 15 Ha and a shifted k-point grid of 4x4x4 mesh was used. The following states were used in the PAW, Ag: 4S, 4p, 4d, 5s; Sn: 4d, 5s, 5p; K: 3s, 3p., 4s; P:3s, 3p, Sb: 4d, 5s, 5p; S: 3s, 3p; Fe: 3s, 3p, 3d, 4s. Table 1 shows the various input used in the calculations.

Table1: Adopted input with references

| | a(Å) | b(Å) | c(Å) |
|---|---|---|---|
| $Ag_2FeSnS_4$ | 5.74[a] | 5.74[a] | 10.96[a] |
| $Ag_2KPS_4$ | 6.6471[b] | 6.6471[b] | 8.1693[b] |
| $Ag_2KSbS_4$ | 6.886[c] | 6.886[c] | 8.438[c] |

[a]Caye et al., (1968), [b]Wu et al., (2009), [c]Schimek et al., (1996)

**Results and Discussion**

The electronic band structure of $Ag_2FeSnS_4$, $Ag_2kPS_4$, and $Ag_2KSbS_4$ are presented in Figures 1a, 1b, and Ic respectively. Figure 1 is a plot of energy against point of high symmetry in the Wigner-Seitz cell. The direction of the plot is along Γ-X-M-P-Γ-M. The Fermi level is marked at zero electron volt (0 eV). The electronic band structure of $Ag_2FeSnS_4$ is shown in Figure 1a. $Ag_2FeSnS_4$ is shown to be semimetallic with conduction band crossing the Fermi level at the X, M points. There is no crossing of the valence band into the conduction band. At the Fermi level there is an intermediate band of conduction and valence band. The energy width of the intermediate band (IB) is about 1.0 eV. There is an intra valence band gap of 1.0 eV preceding the IB and an intra conduction band gap of 0.2 eV after IB. This class of materials have been studied by Rasukkannu et al., (2017). Figure 1b displays the band structure of $Ag_2KPS_4$. The material is predicted to be a semiconductor with a direct band gap of 2.19 eV. The band structure is divided into subbands of varying energy width. The width of the subband of the top of the valence band is 3.2 eV while that at the bottom of the conduction band is 1.2 eV. There is high degeneracy at the X and M point of high symmetry. The band structure of $Ag_2KSbS_4$ is presented in Figure 1c. The electronic band structure of $Ag_2KSbS_4$ is comparable to that of Ag2$KPS_4$. The material is a semiconductor with energy band gap of 1.67 eV, about 0.52 eV less than that of $Ag_2KPS_4$. The subband at the valence maximum has an energy width of 4.2 eV which is about 1.0 eV greater than that of $Ag_2KPS_4$. The subbands in the conduction band are narrower compare to that of $Ag_2kPS_4$. The width of the subband at the bottom of the conduction band is about 0.5 eV, dispersion is seen only at the Γ-Point.

(1a) (1b)

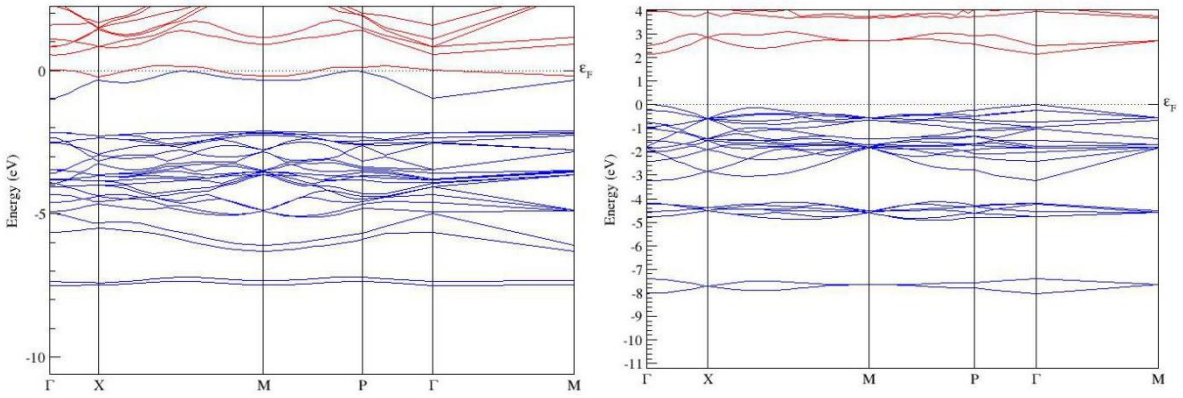


(1c)

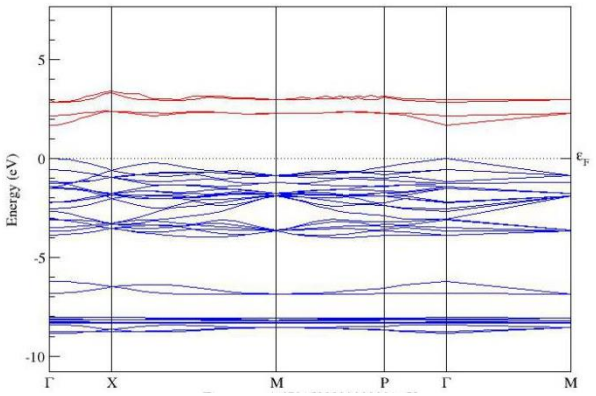


Figure 1: Electronic band structure of (1a) $Ag_2FeSnS_4$ (1b) $Ag_2KPS_4$ and (1c) $Ag_2KSbS_4$.

The density of states (DOS) for $Ag_2FeSnS_4$, $Ag_2KPS_4$, and $Ag_2kSbS_4$ are displayed in figure 2a, 2b, and 2c respectively. The DOS describes the number of states within an energy interval available to be filled by electrons. The plot is DOS in states/Ha/cell against energy in Hartree. Figure 2a shows the DOS for $Ag_2FeSnS_4$, the Fermi level is at 0.21 Ha. The calculation is spin polarized, the feature in black line represents spin-up while the red represents spin–down. Energy feature in the DOS captures the states represented in the band structure. At the Fermi energy, the DOS for spin-up and spin –down are qualitatively and quantitatively the same. Figure 2b displays DOS for $Ag_2KPS_4$ with the Fermi level at 0.2 Ha. The subbands in the valence and conduction band are clearly seen. All features in the band structure are well represented in the DOS. The DOS for $Ag_2KPS_4$ is shown in figure 2c. The Fermi energy is at 0.03 Ha, Again, all features in the band structure are well represented in the DOS. The states between -0.1 Ha and the Fermi level represent the subband at the valence top. The two peaks after the 0.1 Ha mark are the two conduction subband features in the band structure.

(2a) (2b)

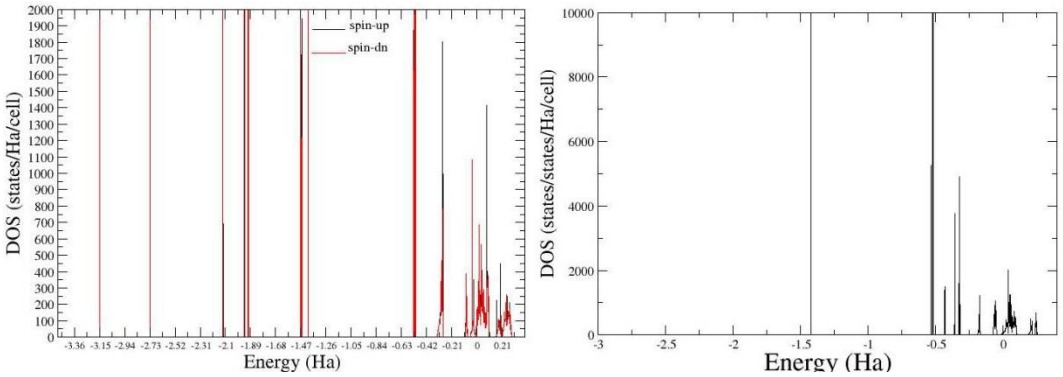


(2c)

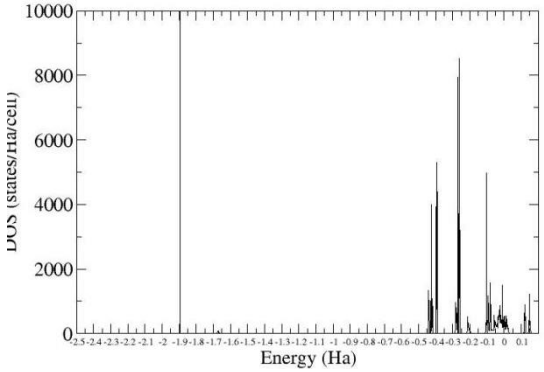


Figure 2: The TDOS for (2a) $AgFeSnS_4$ (2b) $Ag_2KPS_4$ (2c) $Ag_2KSbS_4$

The partial density of states (PDOS) of $Ag_2FeSnS_4$ for all the constituent atoms are shown in Figures 3, 4,5, and 6. The orbital decomposition for silver; Ag-4s, Ag-5s, Ag-4p and Ag-4d are shown in figure 3. The black line features are for Ag-4s and Ag-5s, the red lines represent Ag-4p, while the green lines represent contributions from Ag-4d states. Looking at figure 3, the narrow peak at -2.8 Ha is the contribution to DOS from Ag-4s, the feature of red at -1.4 Ha represent the states contribution from Ag-4p for the silver atom, most of its contribution comes from Ag-4d and Ag-5s states. The feature at about -0.5 Ha, -0.3 are of Ag-4d. The subband at the top of valence band, that is, the features between –o.1 Ha to 0.1 Ha are of the Ag-5s and Ag-4d States. The very top of this subband is mostly Ag-4d while its rear is majorly Ag-5s. There is a very small portion of both states in the conduction band seen at 0.2 Ha to 0.3 Ha.

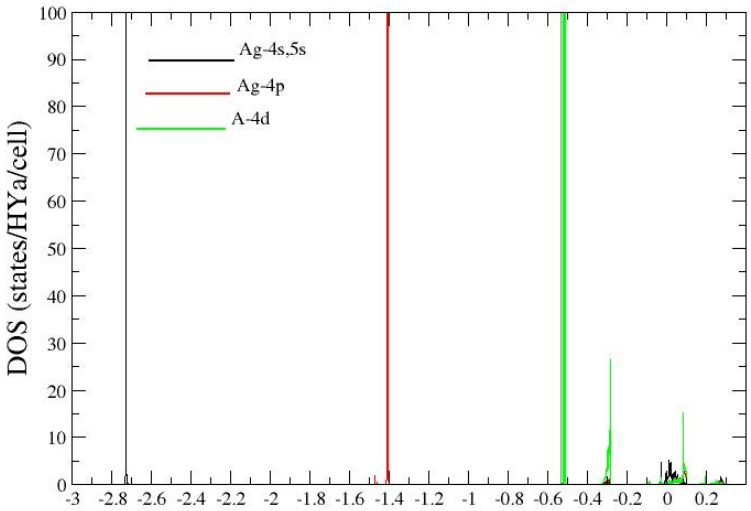


Figure 3: The PDOS of Ag orbitals in $Ag_2FeSnS_4$

The Fe contribution is displayed in Figure 4, as indicated in Figure 4, the black line is for the Fe-5s and Fe -4s states, the red for Fe-3p features while green is for Fe-3d states. At -3.15 Ha is a state corresponding to Fe-3s. The feature at -1.9 Ha corresponds to Fe-3p states. The valence states are represented by the peaks from -0.3 Ha to the Fermi level. The Fermi level is at 0.21 Ha. The IB is made up of Fe-3p and Fe-4s states. Most of Fe contribution in the conduction band are of Fe-4s state, there is a large peak of Fe-4s at about zero marks.

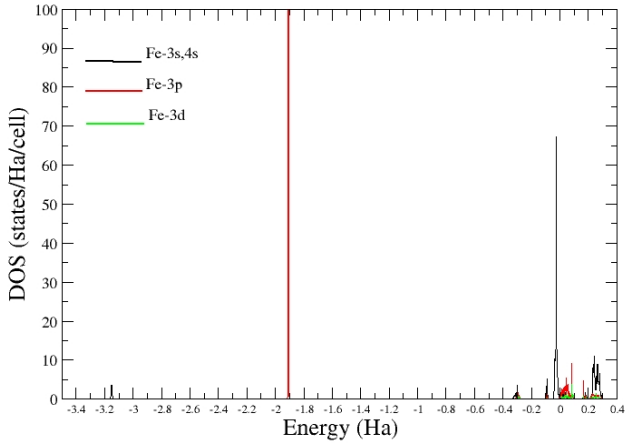


Figure 4: The PDOS of Fe orbitals in $Ag_2FeSnS_4$

The orbital contribution of Tin (Sn) atom to the DOS is presented in Figure 5, as indicate in the graph, features marked in green, black, and red represents contribution from Sn-4d, Sn-5s, and Sn-5p states respectively. Most of the Sn-4d states are at -1.9 Ha. The IB subband has a substantial number of Sn-4s state. The conduction band has all three states with Sn-5p dominating.

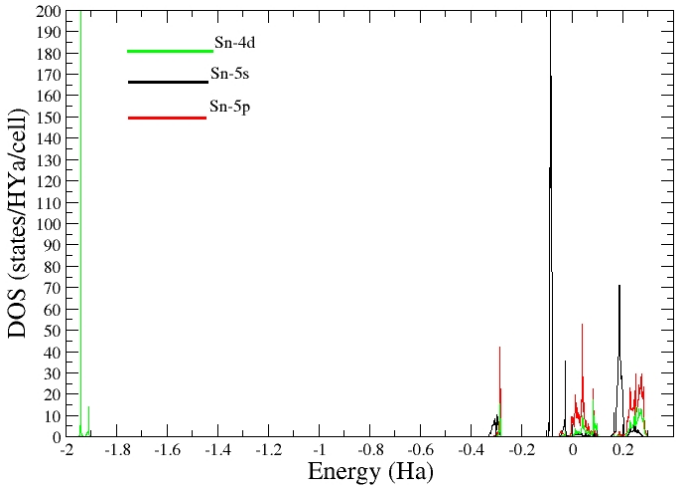


Figure 5: The PDOS of Sn orbitals in $Ag_2FeSnS_4$

S-3s and S-3p contributions are displayed in Figure 6. For sulphur, the top of the valence band is majorly of S-3p. The IB subband also has a significance portion of S-3p. The S-3s contribution is the feature in black at -0.3 Ha. The PDOS for $Ag_2FeSnS_4$ showed S-3p and Sn-5s dominating the IB subband with Sn-5s slightly out numbering S-3p within this energy width. Sn-5s dominated the conduction band.

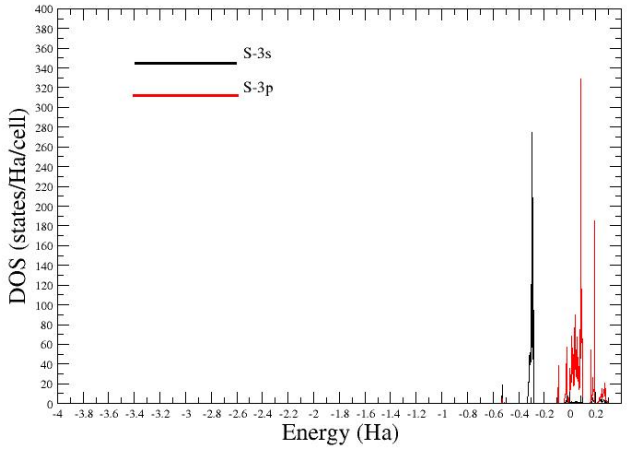


Figure 6: The PDOS of S orbitals in $Ag_2FeSnS_4$

PDOS for $Ag_2KPs_4$ are shown in figure 7 to 10. The contribution from Ag atom are displayed in Figure 7. The black, red and green line feature represents contribution to DOS of Ag-s (4s and 5s) Ag-4p, and Ag-4d respectively. Ag-4s contribution is seen at -2.7 Ha. Silver's contribution to the valence and conduction is the Ag-5s state, most of the valence subbands are Ag-4d states, seen between -0.5 Ha to -0.3 Ha.

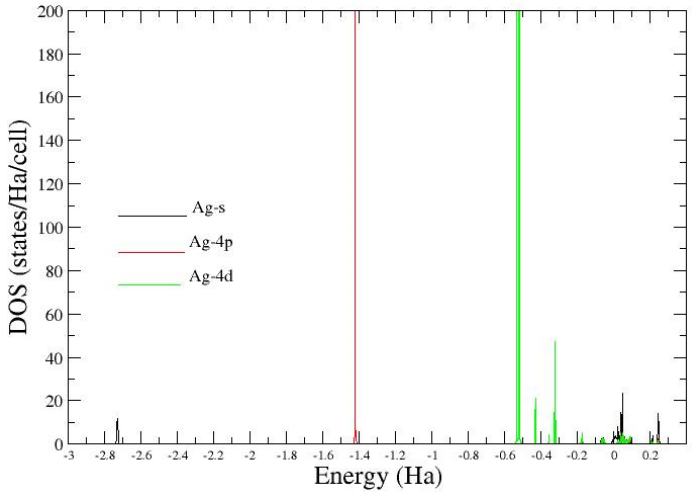


Figure 7: The PDOS of Ag orbitals in $Ag_2KPS_4$

Figure 8 shows the orbital contribution from the K atom. Most of the K-3p state contribution is seen between -0.4 Ha to -0.3 Ha, and K-3p is the dominant state in the valence band.

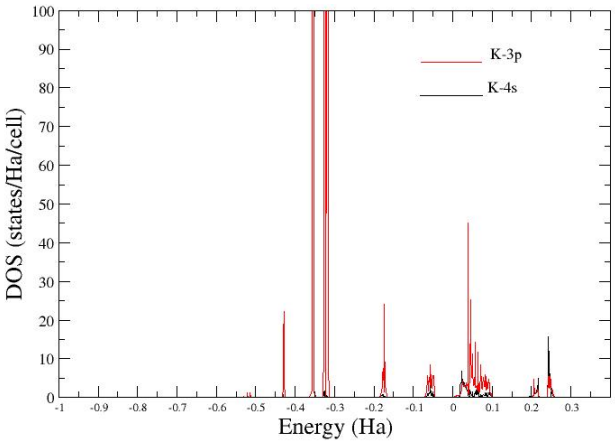


Figure 8: The PDOS of K orbitals in $Ag_2KPS_4$

The contributions from Phosporus (P) atom is presented in Figure 9. The peaks in black are the P-3s state contributions to DOS and they are at -0.5 Ha, between -0.2 and -0.15 Ha. The bottom of the conduction band is predominately P-3s state.

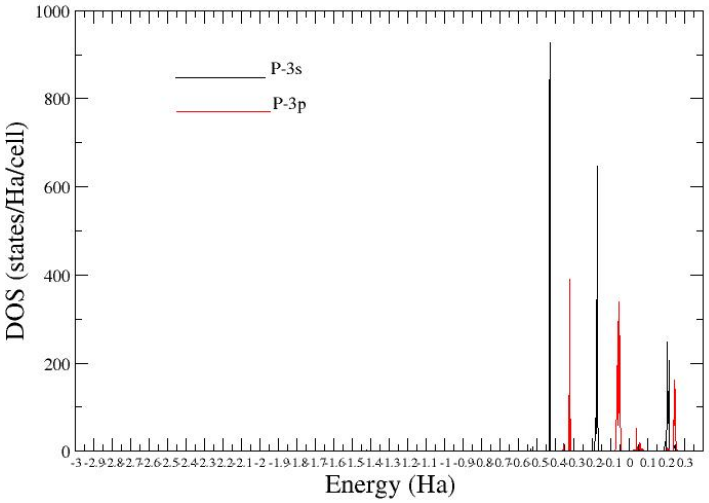


Figure 9: The PDOS of P orbitals in $Ag_2KPS_4$

Sulphur's contribution is displayed in Figure 10. The contribution with the largest peak belongs to S-3s state, and it occurs at –o.33 Ha. The valence band is majorly the S-3p states. For $Ag_2KPS_4$ PDOS, S-3p state dominates the top valence subband while P-3p is the dominant state at the bottom of the conduction band.

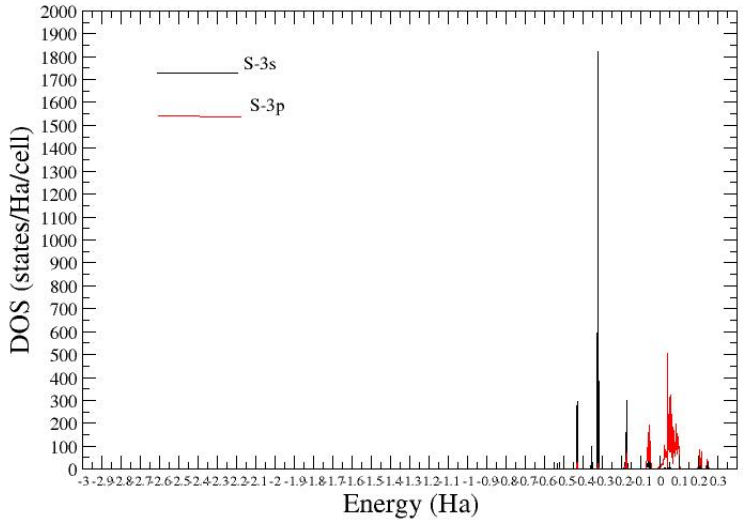


Figure 10: The PDOS of S orbitals in $Ag_2KPS_4$

The PDOS of the elemental component of $Ag_2kSbS_4$ are shown in Figures 11 to 14. The orbitals contribution of the silver atom are presented in Figure 11. Ag-4s state is represented by the small peak at -3.0 Ha, the red line feature at about -1.65 Ha is the contribution of Ag-4p. The Ag-4d states dominates the contributions from Ag atom. The peaks from -0.45 Ha to the Fermi level,

marked in greens are the Ag-4d state contribution. The contribution from Ag-5s is the peak at 0.15 Ha.

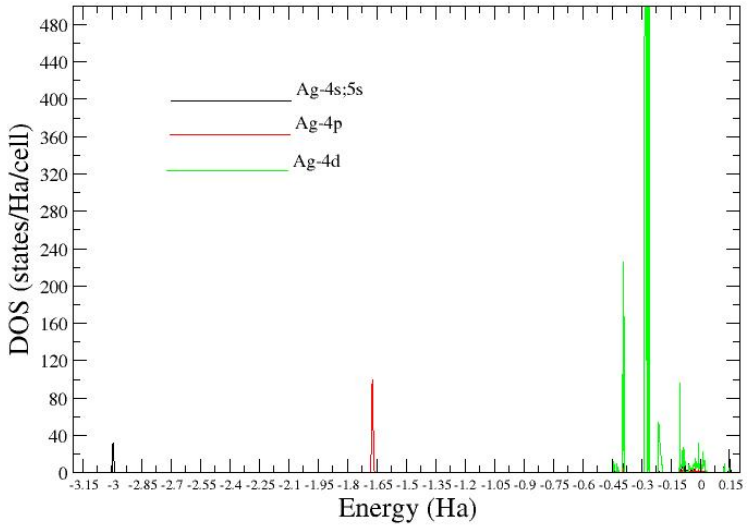


Figure 11: The PDOS of Ag orbitals in $Ag_2KSbS_4$

Figure 12 presents the orbital contributions to DOS from the K contribution. The K-3p states are the dominate contribution from Potassium. This is seen from the energy interval of - 0.45 Ha all the way to Fermi level. Much of K-3p states are concentrated at - 0.45 Ha to - 0.4 Ha. The peak at -1.0 Ha is of K-3s state, K-4s state is the feature in black between - 0.1 Ha and zero mark, and the rear conduction subband at 0.2 Ha.

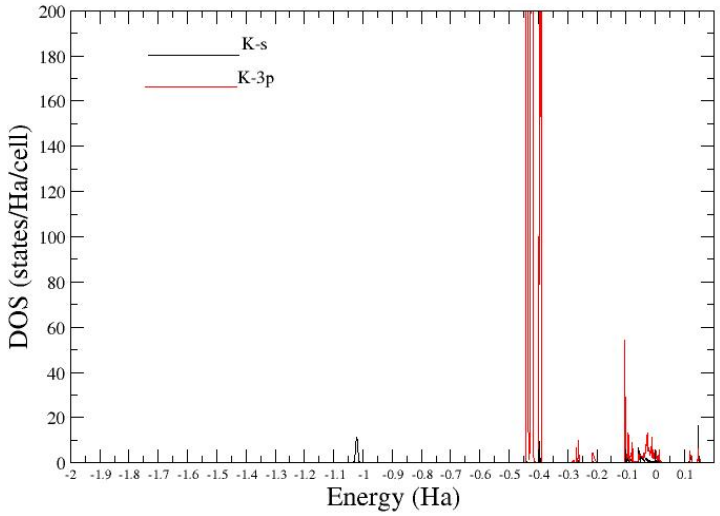


Figure 12: The PDOS of K orbitals in $Ag_2KSbS_4$

The contributions from Sb is shown in Figure 13. The black features of the graph represents the contribution of Sb-5s state, the red from Sb-5p, while the green is from Sb-4d states. The bottom of the conduction band is majorly of the Sb-5s states, while the top of the valance band is of the Sb-5d state. The conduction band has contributions from Sb-5s and Sb-4d states, this is as seen between 0.1 Ha and 0.15 Ha. The top of the valence band is predominantly 5b-4d state.

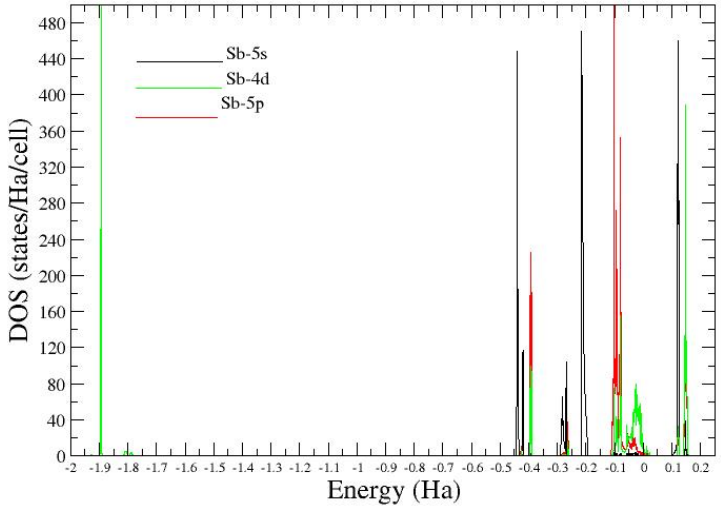


Figure 13: The PDOS of Sb orbitals in $Ag_2KSbS_4$

The sulphur (S) atoms contribution to DOS is displayed in Figure 14. The states at the top of the valence band and at the bottom of the conduction band comes from contributions from 5-3p states. The contributions from S-3s are majorly within the energy interval of - 0.45 Ha to - 0.4 Ha. So for $Ag_2KSbS_4$, S-3p is the dominant state at the valence band maximum while the conduction band bottom is mainly the contributions from Sb-4d and 5b-5s.

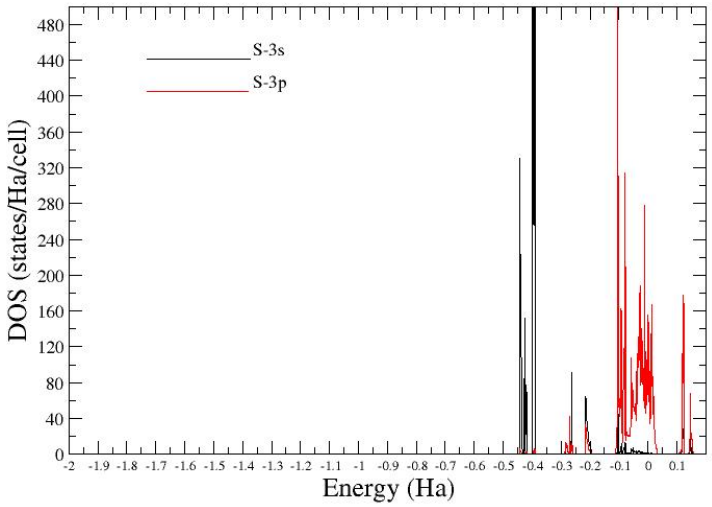


Figure 14: The PDOS of S orbitals in $Ag_2KSbS_4$

## Conclusion

Quaternary chalcogenides are in the spotlight due to their technological applications. Their properties have been investigated experimentally and theoretically. This work was based on the density functional theory, and predicted that $Ag_2FeSnS_4$ is semimetallic, while $Ag_2KPS_4$ and $Ag_2KSbS_4$ are semiconductors with direct band gap.

## References

Berri S., Bouarissa N., Oumertem M., Chami S. (2019), First –principles investigation of structural, electronic, optical and thermodynamic properties of $Ag_2KSbS_4$, Comput Cond. Mat. Vol. 19, e00365. https://doi.org/10.1016/j.cocom.2019.e00365.

Brunetta C. D. , Karuppannam B., Rosmus K. A. , Aitken J. A. (2012), The Crystal and electronic band structure of the diamond –like semiconductor $Ag_2ZnSiS_4$, J. Alloy. Compds, 516: 65-72, DOI:10.1016/j.jallcom.2011.11.133.

Caye P. R., Laurent Y. , Picot P., Pierrrot R. (1968), La Hocratite, $Ag_2SnFeS_4$, Une nourvelle espece minerale, Bull. Soc. Fr. Mineral. Cristallogr. 91, 383-387.

Coleman N., Jr., Liyanage E. A., Lovander M. D., Leddy J., and Gillan E. G. (2022), Facile solvent-free synthesis of metal thiophospates and their examination as hydrogen evolution electrocatalysts, Molecules, 27, 5053, https://doi.org/10.3390/molecules.27165053.

Fuentealba P., Olea C., Aguilar-Bolados H., Audebrand N., De Santana R. C., Doerenkamp C., Eckerts H., Magon C. J., and Spodine E. (2020), Phy. Chem. Chem. Phys. , 202 (16), pp.83150-8324.

Gonze X., Beuken J.-M., Caracas R., Detraux F., Fuchs M., Rignanese G.-M., Sindic L., Verstraete M., Zerah G., Jollet F., Torrent M., Roy A., Mikami M., Ghosez Ph., Raty J.-Y., and Allan D.C., (2002) First-principles computation of material properties : the Abinit software project, Computational Materials Science 25, 478-492.

Gonze X., Rignanese G.-M., Verstraete M., Beuken J.-M., Pouillon Y., Caracas R., Jollet F., Torrent M., Zerah G., Mikami M., Ghosez Ph., Veithen M., Raty J.-Y., Olevano V., Bruneval F., Reining L., Godby R., Onida G., Hamann D. R., and Allan D. C., (2005) A brief Introduction to the Abinit software package. Z. Kristallogr. 220, 558-562.

Hang J., Su X., Hou D., Lei B., Yang Z., and Pan S. (2017), First – principles study lone-pair effects of Sb (III)-S chromophore influence on SHG response in quaternary potassium containing silver antimony sulfides, J. Solid Stat. Chem., Vol. 249, pp215 -220.

Kang L., Zhou M., Yao J., Lin Z., Wu Y., and Chen C. (2015), Metal thiophoshates with good mid-infrared nonlinear optical performances: A first-principle prediction and analysis, J. Am Chem. Soc. 137, 40, 13049-13059.

Lange P. L., Merkle R., Maier J., and Schleid T. (2023), Structure, spectroscopic investigations and discussions on conductivity of rare-earth metal theiphosphates (V) hosting silver ions in the $Ag_2RE(PS4)_2$ series (RE = Y,Dy, Ho and Er), Solid Stat. Sci. Vol. 143, 107280.

Moroz M., Reshetnyak O., Demchenko P, Prokhorenko M., Soliak L, Rudyk B., Pereviznyk O.j and prokhorenko S. (2020), Thermodynamic properties of silver–containing compounds of the Ag-Fe-Sn-S System obtained by low temperature solid –state Synthesis, Ukrainian Chem. J. 86(11), 34-50, https://doi.org/10.33609/2708-129x.86.11.2020-34-50.

Nhalil H., Han D., Du M-H., Chen S., Antonio C. D., Gofryk K., and Saparov B. (2018), Optoelectronic properties of candidate photovoltaic $Cu_2PbSiS_4$, $Ag_2PbGeS_2$, and $KAg_2SbS_4$ semiconductor, Journal of Alloys and Compd. 746, 405-412.

Rasukkannu M., Velauthapillai D., and Vajeeston P. (2017), Computational modeling of novel bulk materials for the intermediate-band solar cells, ACS Omega 2, 1454-1462, DOI:10.1021/acsomega.6b00534.

Schimak G. L, Pennington W.T, Wood P.T.,Wood P.T., Kolis J. W. (1996), Supercritical Ammonia Synthesis and Characterization of four new akali metal silver antimony Sulfides: $MAg_2SbS_4$ and $M_2AgSbS_4$ (M = k, Rb), J. Solid State Chem. Vol. 123, issue 2, pp 277-284.

Wu P., and Bensch W. (2009), Synthesis, crystal structures and spectroscopic properties of $Ag_2Nb(P_2S_6)(S_2)$ and $KAg_2(PS_4)$, J. Solid Stat. Chem, vol. 182, Issue 3, P. 471-478, DOI:10.1016/j.jssc.2008.11.017.

Yajima J., Ohta E, and Kanazawa Y. (1991), Toyohaite, Ag2FeSn3S8, a new mineral, Mineralogical Journal, Vol.15, No 5, pp 222-232.